Zeitschrift: Bulletin des Schweizerischen Elektrotechnischen Vereins
Herausgeber: Schweizerischer Elektrotechnischer Verein ; Verband Schweizerischer Elektrizitätswerke
Band: 51 (1960)
Heft: 20

Artikel: Modern Microwace Travelling-Wave Tubes
Autor: Jenny, H.K.
DOI: https://doi.org/10.5169/seals-917072

Die Fortpflanzungskonstante für Spannung U und Strom I auf der Leitung ergibt sich daraus nach bekannten Regeln zu:

$$\beta^2 = -\left(\mathrm{j}\,\omega\,L_l + \frac{1}{\mathrm{j}\,\omega\,C_l}\right)\mathrm{j}\,\omega\,C_t \qquad (23)$$

Mit Gl. (22) erhalten wir daraus wieder die Gl. (11) für β. Der Wellenwiderstand der Leitung folgt zu

$$Z_w = \frac{\beta}{\omega\,\varepsilon_t} \qquad (24)$$

Negative Werte von ε_t bedeuten eine negative Kapazität C_t und damit einen negativen Wellenwiderstand. Dieser bedingt, dass der Leistungstransport wegen der Phasenumkehr des Stromes $I = U/Z$ in umgekehrter Richtung verläuft wie die Phasengeschwindigkeit. Im Hohlleiter entspricht der Phasenumkehr von I eine solche von $\vec{H}_t$. Die negativen Werte von ε_t werden durch den Leitungsstrom der Plasmaelektronen bewirkt.

Zum Auftreten einer negativen Kapazität sei bemerkt, dass damit nur ein Element beschrieben wird, das die Beziehung zwischen Strom und Spannung gemäss

$$I = C_t\frac{\mathrm{d}\,U}{\mathrm{d}\,t} = \varepsilon_t\frac{\mathrm{d}\,U}{\mathrm{d}\,t} = \mathrm{j}\,\omega\,\varepsilon_t\,U \qquad (25)$$

regelt; bei negativen Werten von ε_t eilt der Strom der Spannung nach. Die in der Kapazität im Zeitmittel gespeicherte elektrische Energie ist nach Gl. (17) durch

$$W_{e\,med} = \frac{1}{4}\cdot\frac{\mathrm{d}}{\mathrm{d}\omega}\,(\omega\,C_t)\,U_{max}{}^2$$

gegeben und stets positiv[6]).

Adresse des Autors:
Prof. Dr. *F. Borgnis*, Schöne Aussicht 13, Hamburg 22 (Deutschland).

Modern Microwave Travelling-Wave Tubes

By *H. K. Jenny*, Harrison

621.385.6

1. Introduction

The almost explosive growth of the electronics field has necessitated the use of increasing portions of the frequency spectrum. Although the range of audio frequencies up to tens of megacycles/second fulfilled the needs of the radio era, the birth of television, radar, and multichannel radio-relay systems demanded greatly expanded frequency ranges. Thus, the requirements for microwave tubes operating at frequencies upward from several hundred megacycles/second became a desperate need. In contrast to the limited operational capabilities of early tubes, the design of microwave tubes today has progressed to the point at which systems of extreme sophistication and complexity, as well as high reliability, are not only possible, but common place.

Perhaps the most promising microwave amplifying device in use today is the *travelling-wave tube*. This paper describes three types of travelling-wave tubes: low-noise tubes, periodic-permanent-magnet-focused medium-power tubes, and electrostatically focused high-power tubes. Tubes of all three types are commercially available today. Furthermore, development results indicate that the systems designer can expect greatly improved versions in the not-too-distant future.

2. The Travelling-Wave Tube

As frequency increases and wavelength decreases, circuit elements become smaller and smaller. Thus, a point is reached at which the physical separation of circuit elements and electron tubes becomes impossible. As a result, most microwave tubes combine circuit and tube elements in one vacuum envelope. Unfortunately, with such an arrangement, circuit elements cannot be altered to meet specific frequency requirements, and the usefulness of a specific tube becomes very much restricted. Usually, conventional microwave tubes can be tuned over frequency ranges of several per cent; the travelling-wave tube, however, is unique in that it is capable of operation over bandwidths in excess of an octave. Moreover, the travelling-wave tube is useful in such applications as amplifiers, oscillators, mixers, frequency multipliers, frequency shifters, noise generators, limiters, phase shifters, frequency devices, and detectors.

Fig. 1 shows the basic elements of the travelling-wave tube. The main circuit consists of a helical slow-wave structure, so-called because it slows down the propagation of the microwave signal in the axial direction and enables efficient energy exchange between the travelling-wave and an electron beam emerging from an electron gun. The beam is contained inside the helix structure by an axial magnetic field which extends from the entrance of the slow-wave structure to the collector. This energy exchange is obtained

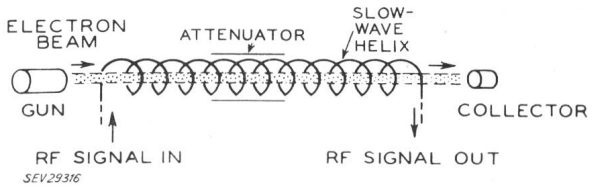

Fig. 1
Basic elements of a travelling-wave tube
Electromagnetic wave travels from left to right along helix

near synchronous conditions, i.e., when the signal propagating velocity is equal to or near the velocity of the electrons in the beam. The input signal reaching the helix modulates the velocity of the electron beam, and, as the beam travels along the helix, this velocity modulation is transformed into density modulation. Energy thus gradually couples back into the helix to leave the tube through the output circuit as an amplified signal. An attenuator placed on the helix prevents feedback from output to input.

3. Low-Noise Travelling-Wave Tubes

Microwave receivers require very-low-noise input amplifiers for high sensitivity, and long-range reception at low transmitter output. Although devices such as masers and parametric amplifiers provide extremely low noise figures

over narrow frequency ranges, the travelling-wave tube heads the list of low-noise, wide-band devices.

Noise figure is defined as the ratio in db of the signal-to-noise power ratios at the input and output of the device. A conventional low-power travelling-wave tube has a noise figure between 20 and 30 db.

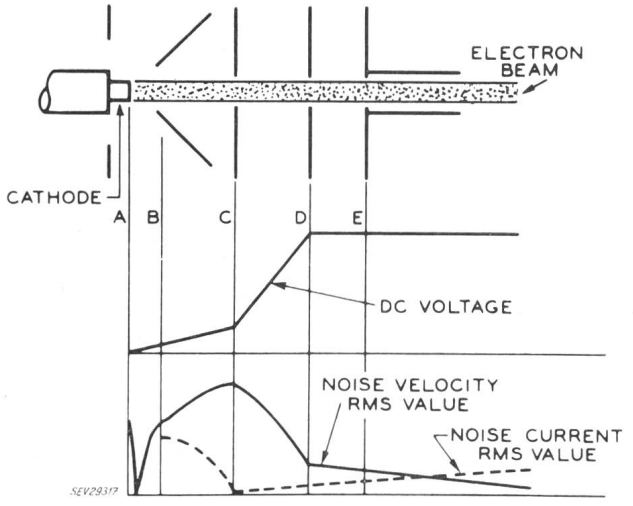

Fig. 2

Drawing showing the exponential potential rise of the electron beam upon passage through parallel-flow low-noise electron gun

A, B, C, D, E Sections

The development of low-noise amplifiers over the last ten years provided an interesting "tug of war" between theory and experimental accomplishments. More than once, the conditions leading to theoretical low-noise minima had to be re-examined in the light of experimental results that provided noise figures lower than the calculated possible values!

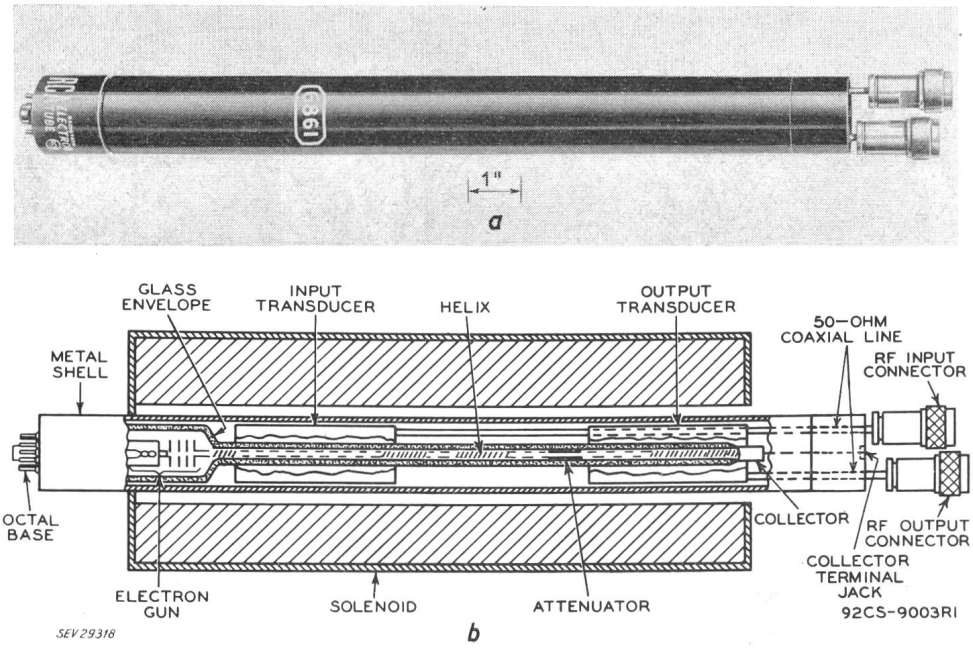

Fig. 3

Type 6861 low-noise travelling-wave tube

a Photograph; *b* Cross-section

During the early 1950's, scientists at Stanford University [1][1]), Radio Corporation of America, and Bell Telephone Laboratories discovered noise in electron beams in standing-wave patterns which could be transformed by changes in applied beam velocity. Through the design of a special gun which transforms the noise wave by means of velocity changes and by a re-positioning of the helix entrance to coincide with a minimum point of the standing wave, a noise figure of the order of 9 db was obtained by *R. W. Peter* [2], as shown in Fig. 2.

Continued refinement of travelling-wave tubes using this type of gun led to the development of the 6861 [3] having noise figures from 5 to 7 db. Fig. 3 shows a photograph and a cross-sectional diagram of the 6861, and Fig. 4 depicts its main performance characteristics—gain, noise figure, power output, and frequency dependence. The 6861 has been in production since 1956 and has destinguished itself through excellent life performance. Zurich Airport, for example, reports that this tube has been operating successfully for 19 800 hours as a pre-amplifier in a radar system.

Recently, research workers have found that further reduction in noise is possible. In addition to the impedance matching from cathode to helix structure by means of multi-electrode guns, several methods of noise suppression are under investigation. These methods vary from reduction of cathode temperature to selection of electrons within limited velocity ranges. Fig. 5 shows the area of noise figures measured to date (shaded) as a function of frequency. Although the effectiveness or the practical application of these schemes has yet to be evaluated, the estimated lower limit for noise figures indicated by the dashed line is expected within the next two years.

In addition to the specific new schemes for noise reduction, a number of additional considerations are necessary. The cathode must have a very dense, thin, and uniform emissive coating and must be capable of operation at low temperature. Extreme care and cleanliness in tube assembly and processing are essential. Very careful gun design is required for a clean, hollow beam and the necessary exponential voltage gradient along the electron gun.

Losses at the input coupler and the helix directly add to the tube noise figure and must be kept to a minimum. A high gain per unit length is desired to keep helix losses low. Because current interception reduces gain and increases noise, the beam must be well focused.

[1]) Refer to the Bibliography at the end of the article.

Present Results

Today, a very active competition for lowest noise achievements is in progress. Fig. 6 shows measurements made by the RCA Microwave Engineering Department in

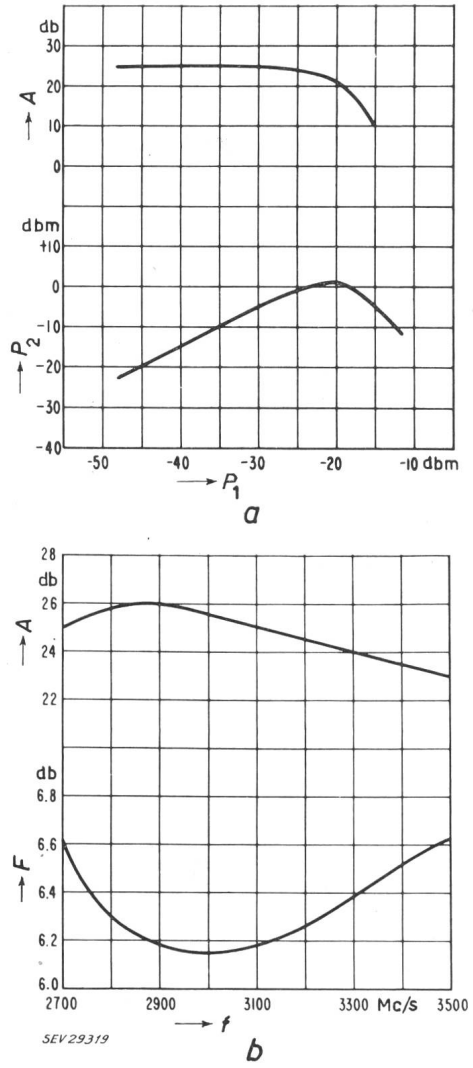

Fig. 4

Characteristics of type 6861 low-noise tube

a Gain A and Power output P_2 vs power input P_1; *b* Gain A and noise figure F vs frequency f; E_f = 5 V; collector voltage = 400 V; helix voltage = 375 V; grid No. 4 voltage = 200 V; grid No. 3 voltage = 40 V; grid No. 2 voltage adjusted to give 150 μA collector current; grid No. 1 connected to cathode at socket; signal frequency = 3100 Mc/s; field strength along helix axis = 525 Gs

Harrison, N. J. The achievement of a 2.5-db tube noise figure represents another milestone in the development of noise-free microwave-amplifier devices. There is little doubt that this figure will be improved as a result of present concerted research and development effort in this area.

4. The Periodic-Permanent-Magnet-Focused Medium-Power Amplifier

The need for small, light, rugged, and reliable microwave amplifiers stimulated the development of the periodic-permanent-magnet-focused travelling-wave tube. Up through the early 1950's, the travelling-wave tube was a fragile thermometer-like device which had to be inserted into heavy solenoids requiring hundreds of watts of energizing power. The system designer suffered veritable nightmares in his attempts to utilize these devices. Today, however, the microwave tube industry is offering a broad line of compact periodic-permanent-magnet tubes.

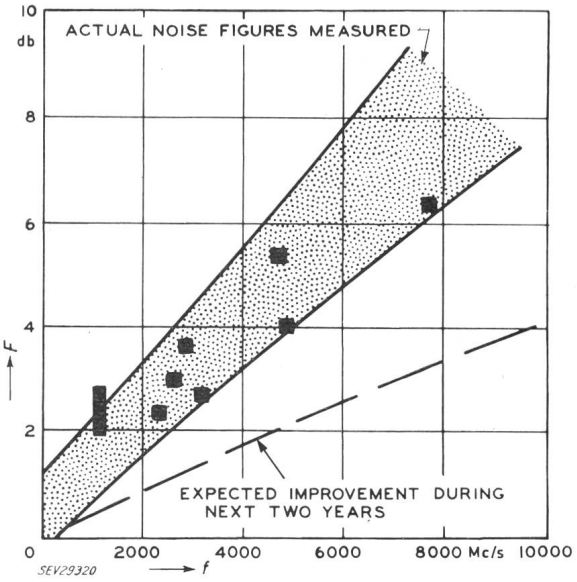

Fig. 5

Noise figure versus frequency

F noise figure; f frequency

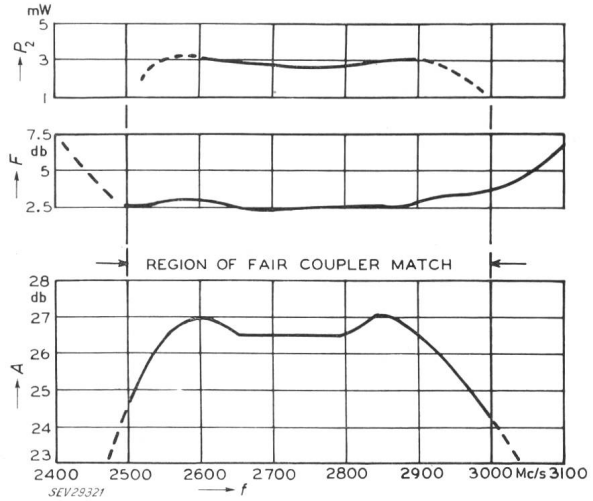

Fig. 6

RCA 6861V gain, power output, and noise figure for optimum operating conditions

f frequency; A gain; F noise figure; P_2 power output

A magnetic field of several hundred gausses is required to focus the travelling-wave-tube beam. Instead of operating within a long uniform field, the beam can be focused equally well by a series of magnetic lenses. Fig. 7 shows how axially polarized ferrite ring magnets and steel pole pieces are alternately stacked to achieve a magnetic field of approximately sine-wave configuration [4; 5].

When a parallel-flow electron beam passes through this structure, it is strongly constrained in the areas of maximum magnetic field and weakly constrained in the areas of weak field. Although the resultant spiraling motion of the individual electrons causes beam scalloping, performance equalling that of a tube operating in a uniform field can be achieved through careful design [6; 7].

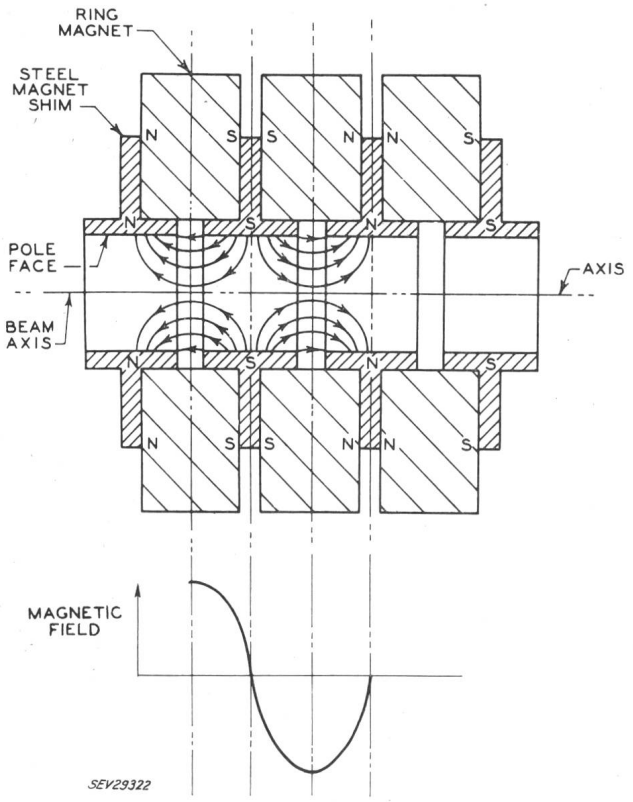

Fig. 7
Cross-section of focusing structure showing ring magnets and steel shims

Typical periodic-permanent-magnet-focused travelling-wave tube package

Fig. 8 shows a photograph and a cross-section of a typical package containing the following components:

a) Pierce-type convergent-flow gun having a control grid,
b) helix slow-wave structure imbedded in fluted-glass envelope,
c) helical input and output couplers,
d) helix-coupled attenuator,
e) collector for depressed-potential operation,
f) ferrite-magnet and steel-pole-piece focusing stack, and
g) metal envelope.

These tube structures are extremely rugged and have withstood severe environmental conditions as follows:

1. Vibration of 5 to 10 *g* at frequencies from 5 to 2000 c/s
2. Shocks of 30 *g*
3. Operation at temperature ranges of from −65 to 100°C
4. Operation at 50000 feet (15000 m) altitude
5. Operation at 100% humidity.

Operating life of these tubes generally reaches many thousand hours.

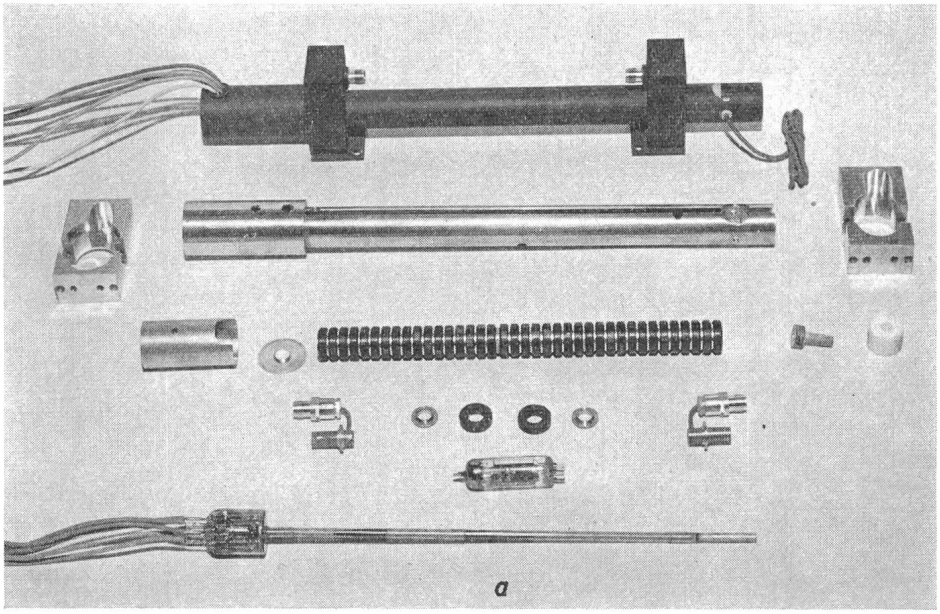

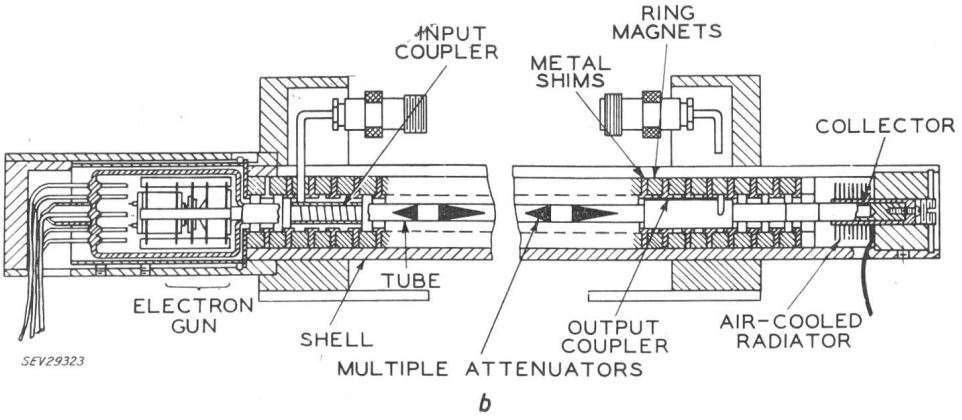

Fig. 8
Components of the RCA-4009 periodic-permanent-magnet travelling-wave tube
a Photograph; *b* Cross-section

Performance

Most of the presently available periodic-permanent-magnet-focused travelling-wave tubes are capable of operation over frequency ranges of up to one octave, and continuing development efforts are constantly improving performance. Fig. 9 illustrates, for example, gain and power-output performance over very wide bandwidth for a tube having the structure shown in Fig. 8.

By no means have the ultimate performance characteristics of these versatile tubes been reached. Many tube types have been "customized" to meet specific requirements. Radio-relay links, for instance, require extreme linearity, good match and low gain variations over relatively narrow bandwidths. Other applications may require wide frequency coverage, flat power output, shaped gain curve and the like.

5. The Electrostatically Focused High-Power Travelling-Wave Tube

The search for methods to improve and simplify microwave amplifying devices has led to the development of a new type of travelling-wave tube, called the Estiatron or elec-

trostatically focused travelling-wave tube. Following *K. Chang's* [8] demonstration of the feasibility of using periodic electrostatic fields in place of the magnetic fields, a double-helix travelling-wave tube utilizing no external magnetic focusing accessories and showing performance similar to that of magnetically focused tubes was developed by *Vaccaro* and *Blattner* [9].

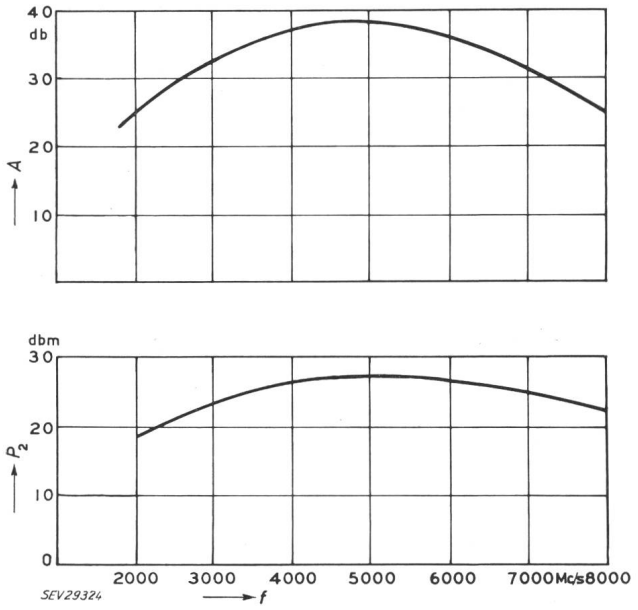

Fig. 9

Gain A and power output P_2 versus frequency f of tube similar to that shown in Fig. 8

Several methods of electrostatic focusing are now being studied. Fig. 10a shows focusing by means of a series of electrostatic lenses formed by rings or discs held alternately at high and low voltage potentials. The electrostatic field between the electrodes produces forces on the electrons, as shown by the arrows in the drawing. Near the low-voltage electrode the electrons move slowly and are directed towards the tube axis. Near the high-voltage electrode they move faster and are directed away from the axis. Because the beam electrons spend more time in that part of the field that pushes them towards the axis, the over-all effect is one of inward movement which balances the space-charge forces to spread the beam.

Another method utilizes "Harris flow" as shown in Fig. 10b. A magnetic field in the gun region causes an annular beam to rotate. The centrifugal force of rotation of the electrons is balanced by a strong radial electrostatic field between the helix and an axial electrode which is at a positive potential with respect to the helix.

Fig. 10c illustrates a third electrostatic focusing method, called "Slalom focusing", which makes use of the fact that among equipotential fields surrounding a parallel array of wires between two planes there is only one pair of continuous equipotential surfaces which intersect between the wires. A ribbon beam launched in the right direction with the right velocity will follow this surface.

An example of how electrostatic focusing can be applied to a high-power travelling-wave tube was demonstrated by the development of a pulse amplifier capable of providing several kilowatts of power output at 9000 Mc/s.

The slow-wave circuit

Because frequency and power-output levels of high-power electrostatically focused tubes make a helix unsuitable as a slow-wave structure, a periodically loaded waveguide structure has been developed [10]. A waveguide basically represents a high-pass filter which propagates energy having a phase velocity higher than the velocity of light at

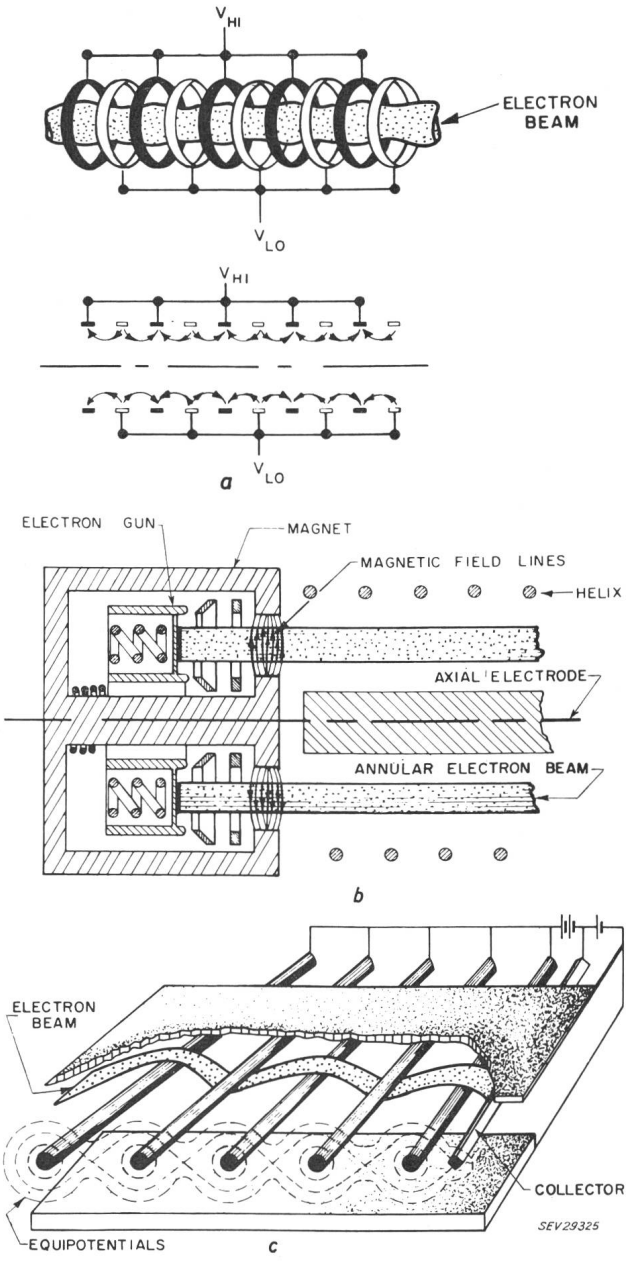

Fig. 10

Methods of electrostatic focusing

a Electrostatic focusing of an electron beam flowing through a series of rings held at alternately high and low potentials and the forces on an electron due to the electrostatic field
V_H high potential; V_L low potential
b "Harris flow" focusing of an annular electron beam
c "Slalom" focusing of an electron beam

all frequencies. If the waveguide is loaded with periodically spaced obstacles reflections occur at their locations. Total reflection represents a stop-band and transforms the high-pass filter into a bandpass filter.

The *Brillouin* diagram, also called the ω-β (frequency vs phase) diagram, clearly shows the properties of such

circuits. Rather than a waveguide loaded with periodic obstacles, the individual sections of the waveguide may be regarded as resonant cavities coupled to each other through the obstacles. Thus, as shown in Fig. 11, coupling the

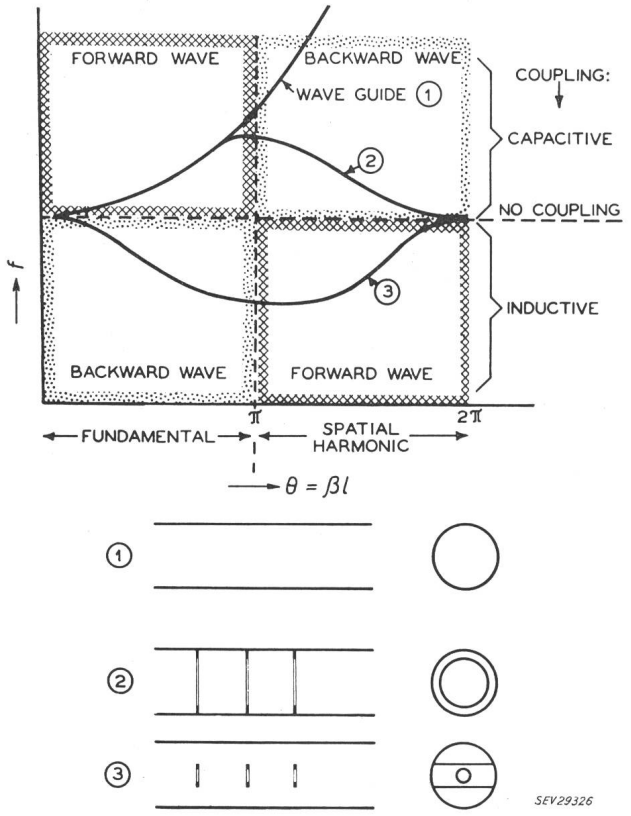

Fig. 11

Delay line characteristics (top) for three different types of line (bottom)

f frequency; $\Theta = \beta l$ phase

cavities through circular slots (capacitive coupling) produces fundamental forward-wave interaction (phase and group velocity have the same sign), whereas coupling with inductive slots produces fundamental backward-wave interaction (phase and group velocity have opposite signs).

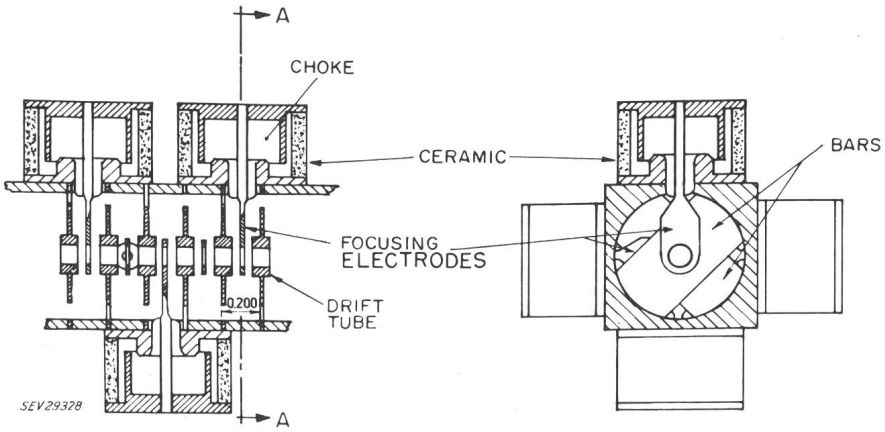

The circuit chosen for this application is similar to example 3 in Fig. 11 and is detailed in Fig. 12. Electrostatic lenses are formed by means of additional focusing electrodes inserted in the cavities in such a manner that they do not interact with the electric fields nor influence the propagating wave. The additional set of electrodes must be isolated from the structure to provide the two potential levels necessary for the focusing lenses. As shown in Fig. 13, this isolation is accomplished by mounting the focusing electrodes on choke sections. Fig. 14 shows a photograph of the module consisting of one lens, a number of these modules are then stacked together to form the complete structure.

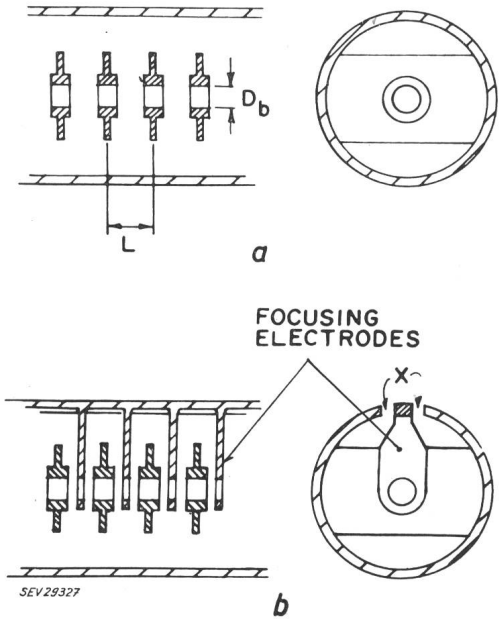

Fig. 12

Round waveguide with periodically spaced bar

a Basic slow-wave structure; *b* Focusing electrodes inserted; D_b bar diameter; L spacing; x air gap

The frequency vs phase diagram of Fig. 15 shows that the addition of focusing electrodes does not disturb the performance of the structure.

Beam focusing

A study comprising both theoretical and experimental phases was conducted to determine voltage distribution for optimum beam focusing. The objective of the study was to discover a method for focusing a beam of high perveance having minimum scalloping with a minimum voltage differential between electrodes.

Fig. 16 shows the ideal electrode arrangement for focusing a laminar, parallel-flow beam and the potential distribution with and without space-charge effects. The optimum condition (i.e., when a maximum of current is transmitted through the lenses) is given by:

$$\left.\frac{dV}{dZ}\right|_{Z=0} = 0$$

where V = potential, Z axial coordinate

and is shown by the broken line. The electrode shapes

Fig. 13

Crossed-bar structure with focusing electrodes individually supported by choke sections

satisfying this condition were obtained by electrolytic tank measurements. The angle Θ increases with the ratio of beam diameter to focusing-electrode diameter.

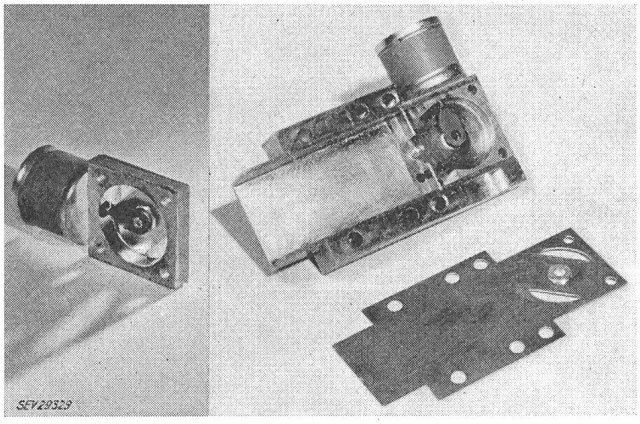

Fig. 14
A single module (left) and a partially brazed coupling section (right)

Tube evaluation

Many questions arose as to the performance of this type of device operating under large-signal conditions when rf and focusing potentials become comparable in size. Of particular concern was the behavior of the large-signal-modulated beam passing through alternating accelerating and decelerating dc fields. *W. Siekanowicz* [11] carried out a theoretical analysis showing that two modes of operation

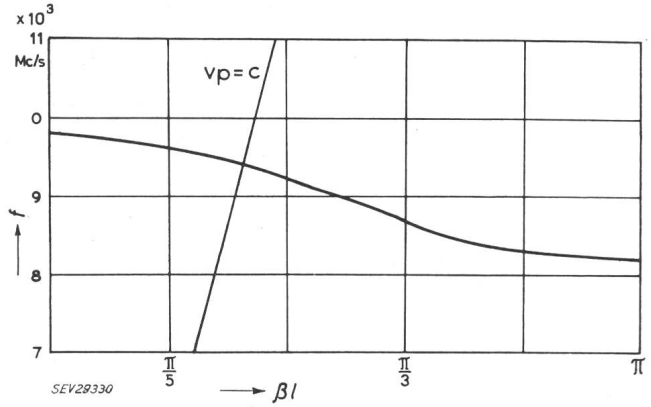

Fig. 15
Frequency f vs phase βl diagram of a cross-bar structure with choke supported focusing electrodes
v_p phase velocity c velocity of light

are possible. When the bars of the cavities are operated at low voltage and the focusing electrodes at high voltage, the tube gain is higher than in the comparable case utilizing magnetic focusing. With the reverse condition (i.e. operating bars at high potential and focusing electrodes at low potential), the gain decreases. These effects are shown quantitatively by computation of the beam coupling coefficient.

Fig. 17 shows a schematic drawing of the complete tube as it was tested, and Figs. 18a, b and c show actual test results.

These measurements were made on a short tube structure having no attenuation of the delay line. Subsequent tests will be made on longer structures to obtain gain values in excess of 30 db and will require internal isolation by means of an attentuator.

The following is a summary of the test results:

Peak power output	10 kW
Small-signal gain	16 db
Small-signal gain per cell	2.3 db
Bandwidth	10 %
Efficiency	33 %
Bar voltage	9 kV
Focusing-electrode voltage	30 kV
Collector current	3 A
Beam-transmission efficiency	86 %

The collector of this tube is operated at the lower (bar) voltage. Thus, high efficiency is actieved and no additional voltages are required other than those needed to operate a conventional travelling-wave tube.

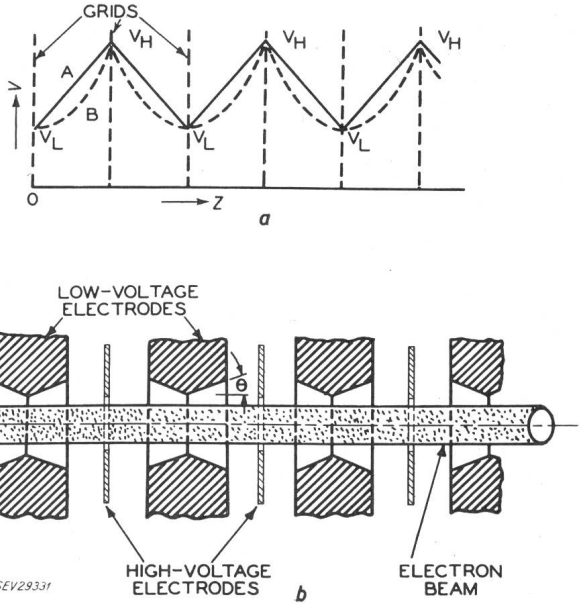

Fig. 16
Ideal electrode arrangement for focusing a laminar, parallel-flow beam
a DC voltage distributions used for evolution of the ideal electrostatically-focused electron beam
b Practical electrodes used for approximating the ideal dc voltage distribution for electrostatic beam focusing
V Voltage; Z axial coordinate
A straight-line approximation; B actual distribution; V_H high potential; V_L low potential; Θ angle

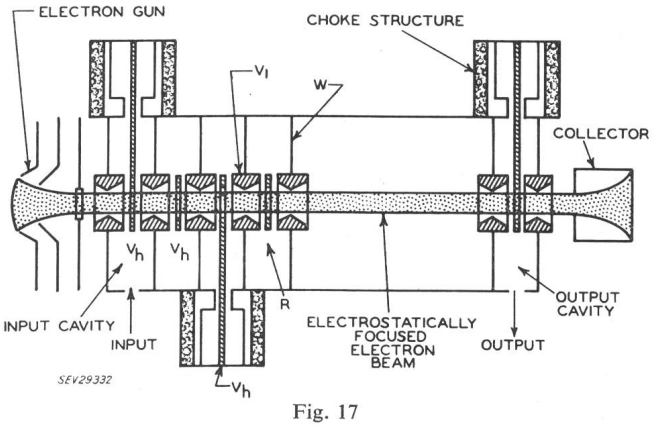

Fig. 17
Schematic representation of an electrostatically focused beam type amplifier employing ideal focusing electrodes
V_l low potential; V_h high potential;
R Resonator; W Resonator wall

6. Summary

Low-noise travelling-wave tubes

Commercial types operating with noise figures of from 5 to 6 db are available today. In the laboratory, however, measurements of 2.5 db noise figure have been achieved, with theoretical studies indicating further decreases. Thus, the travelling-wave tube is a match for parametric amplifiers for use in microwave receivers, and becomes the preferred type whenever appreciable bandwidths are required.

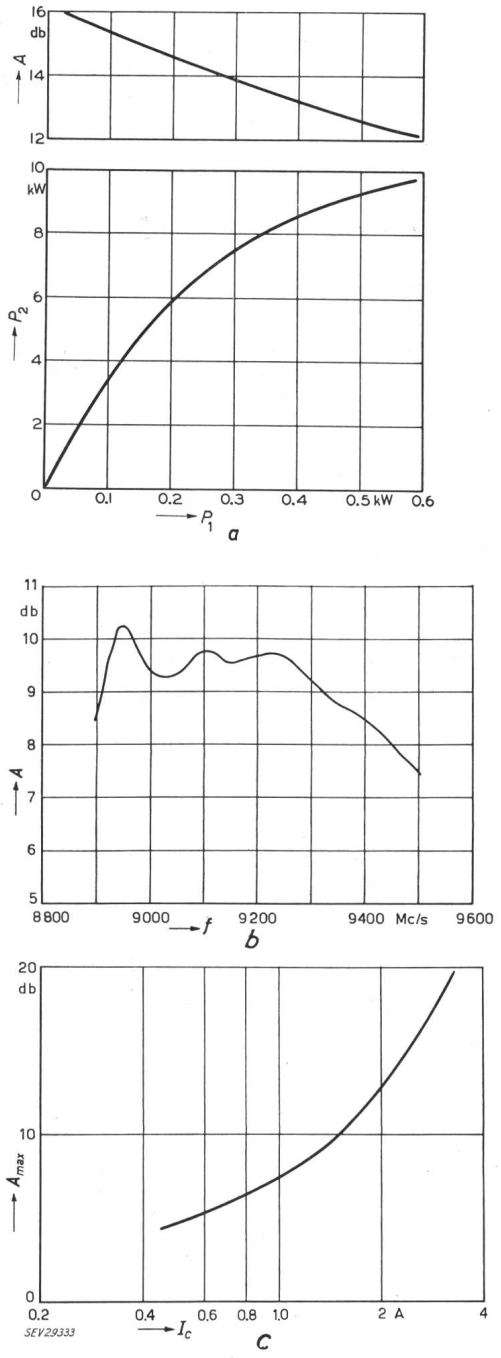

Fig. 18

Test results with tube type shown in Fig. 17

a RF peak power output P_2 and gain A as a function of RF peak power input P_1
Frequency = 9000 Mc/s; focusing-electrodes voltage = 31.6 kV; drift-tube voltage = 10.4 kV; peak dc collector current = 3 A; beam transmission efficiency: without RF drive = 86%, with RF drive = 76%

b Small-signal P_1 gain A as a function of frequency f
Drift-tube voltage: 7.5 kV; focusing-electrodes voltage = 26 kV; peak dc collector current: 1,5 A

c The maximum small-signal gain A_{max} as a function of peak dc collector current I_c
Frequency = 9000 Mc/s; $\frac{\text{dc voltage of focusing electrode}}{\text{dc voltage of drift tubes}} = 3.3$

Periodic-permanent-magnet medium-power travelling-wave tubes

These small, light, and rugged packages are rapidly becoming the "workhorses" of the microwave equipment designer because of their versatile nature. Operation over frequency ranges of several octaves and gain values in excess of 50 db are expected in the near future.

Electrostatically focused high-power travelling-wave tubes

The Estiatron is the youngest member of the travelling-wave tube family and distinguishes itself through several advantages over other microwave amplifiers:

1. Smaller size and weight
2. Operation over wider environmental ranges (temperature, vibration)
3. Longer life as a result of freedom from ion oscillations and ion bombardement of cathode
4. Improved interaction between beam and circuit (increased gain and power)
5. Depressed-collector operation for high efficiency
6. No additional voltages over those required for conventional travelling-wave tubes.

The electrostatically focused tube, however, requires more care in design and processing because of the voltage difference between adjacent circuit and focusing electrodes.

The frequency range of 100 to 2000 Mc/s is particularly attractive for extremely small and light helix-type Estiatrons. A number of different slow-wave structures are suitable for Estiatrons yielding megawatts of peak ouput power. Moreover, the performance of power tubes at 9000 Mc/s amply demonstrates that these tubes are not restricted to the lower frequency ranges. Other extremely promising results on both low- and high-power Estiatrons indicate that this type will not only replace conventional travelling-wave tubes in a number of applications but will also fill new requirements not heretofore achievable.

Bibliography

[1] *Watkins, D. A.:* Traveling-Wave Tube Noise Figure. Proc. IRE Vol. 40(1952), No. 1, p. 65...70.

[2] *Peter, R. W.:* Low-Noise Traveling-Wave Amplifier. RCA Rev. Vol. 13(1952), No. 3, p. 344...368.

[3] *Kinaman, E. W.* and *M. Magid:* Very Low-Noise Traveling-Wave Amplifier. Proc. IRE Vol. 46(1958), No. 5, Part. I, p. 861...867.

[4] *Mendel, J. T., C. F. Quate* and *W. H. Yocom:* Electron Beam Focusing with Periodic Permanent Magnet Fields. Proc. IRE Vol. 42(1954), No. 5, p. 800...810.

[5] *Chang, K. K. N.:* Optimum Design of Periodic Magnet. Structures for Electron Beam Focusing. RCA Rev. Vol. 16(1955), No. 1, p. 65...81.

[6] *Siekanowicz, W. W.* and *F. Sterzer:* A Developmental Wide-Band, 100 Watt, 20 DB, S-Band Traveling-Wave Amplifier Utilizing Periodic Permanent Magnets. Proc. IRE Vol. 44(1956), No. 1, p. 55...61.

[7] *Sterzer, F.* and *W. W. Siekanowicz:* The Design of Periodic Permanent Magnets for Focusing of Electron Beams. RCA Rev. Vol. 18(1957), No. 1, p. 39...59.

[8] *Chang, K. K. N.:* Biperiodic Electrostatic Focusing for High-Density Electron Beams. Proc. IRE Vol. 45(1957), No. 11, p. 1522...1527.
[9] *Blattner, D. J.* and *F. E. Vaccaro:* Electrostatically Focused Traveling-Wave Tube. Electronics Vol. 32(1959), No. 1, p. 46...48.
[10] *Belohoubek, E.:* Propagation Characteristics of Slow-Wave Structures Derived from Coupled Resonators. RCA Rev. Vol. 19(1958), No. 2, p. 283...310.
[11] *Siekanowicz, W. W.* and *F. E. Vaccaro:* Periodic Electrostatic Focusing of Laminar Parallel-Flow Electron Beams. Proc. IRE Vol. 47(1959), No. 3, p. 451...452.

Author's address:
H. K. Jenny, Manager, Microwave Engineering, Electron Tube Division, Radio Corporation of America, Harrison, N.J. (USA).

Über die Verstärkung von Mehrkreis-Klystrons

Von *H. Hagger*, Zürich

621.385.624

1. Einleitung

Bei Laufzeitröhren nach dem Klystrontypus wird die Elektronenstrahlgeschwindigkeit durch eine Wechselspannung über dem Eingangsresonatorspalt beeinflusst. Überlässt man diesen so modulierten Strahl in einem abgeschirmten Driftrohr über eine bestimmte Strecke sich selbst, so entsteht aus der ursprünglichen Geschwindigkeitsmodulation eine Dichteänderung im Strahl, welche beim Durchtritt durch einen zweiten Spalt eine Spannung zu induzieren vermag. Nach dieser Betrachtungsweise lässt sich für das Zweikreis-Klystron eine elektronische Steilheit S_e als Verhältnis von influenzierendem Strom des Ausgangsspaltes und modulierender Spannung über dem Eingangsspalt definieren:

$$S_e \equiv M_2 \frac{i_2(\omega)}{U_1(\omega)} \tag{1}$$

worin

S_e elektronische Steilheit;
i_2 Strom des Ausgangsspaltes;
M_2 Ausgangsspaltfaktor;
U_1 Spannung über dem Eingangsspalt.

Ist $Y_2(\omega)$ der totale Parallel-Leitwert über dem Ausgangsspalt, so folgt für die Verstärkung des Zweikreis-Klystrons:

$$v = \frac{U_2(\omega)}{U_1(\omega)} = -\frac{S_e(\omega)}{Y_2(\omega)} \tag{2}$$

worin

v Spannungsverstärkung;
U_2 Spannung über dem Ausgangsspalt;
Y_2 totaler Parallel-Leitwert über dem Ausgangsspalt.

Nach bekannten Theorien [1; 2][1]) ist es möglich, sowohl S_e als auch Y_2 zu berechnen. Nimmt man nun an, dass die Anregung des k-ten Resonators nur von der Spannung über dem (k-1)-ten Spalt abhängt, so kann man das n-Kreis-Klystron als Kaskadenschaltung von $(n-1)$ Zweikreis-Klystrons auffassen.

In diese Theorie geht als wichtiger Parameter das Verhältnis von Hochfrequenzspannung über dem ersten Spalt zu Strahlbeschleunigungsspannung ein. Diese Grösse ist von vornherein nicht bekannt und kann im allgemeinen erst rückwärts aus einer Optimalbedingung bestimmt werden.

Es gibt nun aber noch einen andern, scheinbar komplizierteren Weg, die Verstärkung eines n-Kreis-Klystrons zu berechnen. Er besteht in der direkten Lösung des Randwertproblems der Maxwellschen Gleichungen für den Elektronenstrahl in einer Struktur mit periodischem Aufbau [3].

[1]) Siehe Literatur am Schluss des Aufsatzes.

Im Folgenden sollen einige Mehrkreis-Klystrons, deren geometrische Daten aus der Literatur vorliegen, und die auf Grund bekannter Theorien berechnet worden sind, nach der Theorie von *Derfler* durchgerechnet und die Ergebnisse mit den angegebenen theoretischen und experimentellen Daten verglichen werden.

2. Elektronische Theorie [1; 2]

Der Parallel-Leitwert Y_2 setzt sich im Resonanzfalle aus drei Anteilen zusammen:

a) dem Leitwert der äusseren Last Y_L;
b) der Belastung durch den Elektronenstrahl Y_B und
c) dem Verlustleitwert des Resonators Y_R.

Von diesen Grössen bedarf nur die Belastung durch den Elektronenstrahl näherer Untersuchung, da die beiden andern Anteile durch den Resonator und die Auskopplung bekannt sind.

Am Rande sei vermerkt, dass $Y_B \equiv G_B + jB_B$ eine komplexe Grösse ist. Die elektronische Verstimmung B_B soll hier nicht weiter betrachtet werden. Drückt man alle geometrischen Grössen in Laufwinkelkoordinaten aus, die aus den Abmessungen durch Multiplikation mit ω/v_0 hervorgehen, so ergibt sich für die reelle elektronische Belastung G_B [1]:

$$G_B = \frac{1}{2Z_0} \cdot \frac{\sin^2 \frac{D}{2}}{\left(\frac{D}{2}\right)^2} \left[1 - \frac{D}{2} \operatorname{ctg} \frac{D}{2}\right] \tag{3}$$

worin

$$Z_0 = U_0/I_0$$

U_0 Beschleunigungsspannung;
I_0 Strahlstrom;
$D = (\omega/v_0)\, d$ Klystronspaltlaufwinkel;
ω Signal-Kreisfrequenz;
v_0 Strahlgeschwindigkeit;
d Klystronspaltbreite.

In Gl. (1) wurde die elektronische Steilheit S_e definiert. M_2 war der Spaltfaktor des Ausgangsspaltes und stellt nichts anderes dar als der Koppelkoeffizient zwischen Strahl und Resonator. Er berechnet sich zu:

$$M_2 = \frac{\sin \frac{D}{2}}{\frac{D}{2}}$$

Den Strom $i_2(\omega)$ gewinnt man durch Fourier-Analyse des Stromimpulses des dichtemodulierten Elektronenstrahles am Ausgangsspalt, während $U_1(\omega)$ aus einer Optimalbedingung für beste Dichtemodulation folgt. Ist ferner